Journal of Solid State Chemistry **152,** 460–465 (2000)
doi:10.1006/jssc.2000.8713, available online at http://www.idealibrary.com on IDEAL®

Ba_3SiI_2, a Double Salt of Barium Iodide and the Zintl Phase Ba_2Si

Steffen Wengert[1] and Reinhard Nesper

Laboratorium für Anorganische Chemie, Eidgenössische Technische Hochschule Zürich, Universitätstrasse 6, CH-8092 Zürich

Received December 14, 1999; in revised form March 6, 2000; accepted March 10, 2000

Reacting Ba_2X (X = Si, Ge) with a melt of BaI_2, new compounds of the composition Ba_3I_2X were found. These are the simplest representatives of double salts between Zintl phases and halides. The isotypic structures were refined by single-crystal X-ray data (*Fddd*, $a = 10.057(2)$, $b = 14.064(3)$, $c = 29.526(4)$ Å, $R/R_w = 0.04/0.07$ for $X = Si$, and $a = 10.064(2)$, $b = 14.082(2)$, $c = 29.605(4)$ Å, $R/R_w = 0.03/0.07$ for $X = Ge$). Magnetic measurements show Ba_3I_2Si to be diamagnetic with a mol susceptibility of 7.7×10^{-5} cm^3/mol. This is in accordance with conductivity measurements and LMTO band structure calculations which show a semiconducting behavior with an electronic band gap of about 0.4 eV.

1. INTRODUCTION

A large amount of research on Zintl phases of silicon has been carried out in the past 20 years. Thereby, a considerable number of interesting novel anionic silicon clusters has been found, most of which have no counterpart in molecular chemistry up to now. Existence and bond topology of these clusters in the solid state is usually rationalized by the so called Zintl Klemm (ZK) concept (1–4). Thus, the electropositive metals (e.g., alkaline earth metals) are considered acting merely as electron donors to their electronegative partners (e.g., silicon). The latter then form covalent bonds, if necessary, to satisfy their octets yielding anionic clusters, chains, layers, and networks (5). Quantum chemical calculations showed that the electronic structure of a Zintl phase is quite well understood only with respect to the electronic states of these anionic clusters and thus affirm the value of the simple concept (5–7).

In the recent years there is a rising interest in using Zintl phases as precursors for subsequent chemical reactions in order to explore the rich chemical potential of this class of compounds. Already the first investigations of E. Zintl about 70 years ago (8, 9) showed that it is possible to dissolve binary phases like Na_4Sn_9 or Na_4Pb_9 in liquid ammonia. The intensively colored solutions contain polyanions of the type E_x^{n-} (E = Sn, Pb), later called Zintl anions. In the meantime various Zintl phases have been studied with respect to their solubilities in different solvents (10–17). However, in all successfully studied cases the charge per atom n/x of the homonuclear clusters E_x^{n-} is below one. Hence the huge number of yet known Zintl anions with $n/x > 1$, especially those of group 14, could not be stabilized in solutions. We decided to investigate salt melts in particular alkaline earth halides with respect to their use as solvents for Zintl phases. Salt melts show higher polarizabilities and should thus be able to stabilize Zintl anions of higher charges. While the flux technique is a common tool in preparative solid state chemistry which is widely used to grow single crystals of oxides, halides, borides, carbides, or chalcogenides out of salt or metal melts (18), the use of salt melts as solvents for chemical reactions has not gained broad entrance in synthetic chemistry up to now. Copper halides have shown to be rather good *solid solvents* for numerous polymeric neutral or low charged main group clusters (19–27). Sundermeyer *et al.* have been studying over years quite intensively the use of salt melts in inorganic synthesis within the temperature range of 100–800°C and developed interesting industrial applications (28–31). Special interest has been focused on the salt chemistry of aluminum halides since they form low melting liquids with good thermal stabilities (32, 33). With the discovery of new room temperature ionic liquids in the last few years, salt melts are also gaining rising interest in the field of organic synthesis (34). Investigating the reactivity of nitridoborates with halogenides of alkaline earth and rare earth metals a number of novel mixed compounds containing both Zintl anions like BN_2^{3-} and halogenide anions were characterized (35–37). The existence of these compounds is an indication for the mobility of BN_2^{3-} anions in the salt melt. Transferring this concept to Zintl phases of group 14, we found a cation exchange by reacting $CaSi_2$ with $SrCl_2$ which resulted in $SrSi_2$ and $CaCl_2$ (38). Thus it should be possible to use salt melts as reaction media for Zintl phases. Numerous of our own investigations have shown that highly charged Zintl anions like those in many silicides and germanides exhibit a delicate balance between the coulomb field provided by the cation surrounding and electronic

[1] To whom correspondence should be addressed. E-mail: wengert@inorg.chem.ethz.ch.

0022-4596/00 $35.00

structure of the anion. Consequently, the loss of coulomb stabilization must result in a severe reconstruction of such anions accompanied by a charge reduction eventually even to the elemental state. Thus, salt melts have to be considered as ideal solvent for such compounds because they are in this respect just comparable or even superior to the pure solid compound. As solid double and triple salts can be understood under the same terms, it may be possible to stabilize even higher charged anions in such phases than in the pure Zintl compound. We will come back to this point later. Recently, Simon *et al.* reported halogenide silicides of rare earth metals containing silicon clusters and halogenides (39, 40) which support this ideas.

Exploring the reactivity of Zintl phases of silicon in halide melts, we were able to synthesize a series of novel double salts.[2] In the following work we will present the compounds Ba_3I_2Si and Ba_3I_2Ge which belong to this new family. With respect to the stoichiometry as well as to their crystal structure, the compounds may be understood as double salts of BaI_2 (42) and the Zintl phases Ba_2Si (43) or Ba_2Ge (44), respectively. Thus Ba_3I_2Si and Ba_3I_2Ge are the simplest representatives of corresponding double salts. The existence of such double salts between Zintl phases of silicon may be considered as chemical proof for the validity of the term Zintl anion in the sense of a real chemical species.

2. EXPERIMENTAL SECTION

2.1. Syntheses

All reagents and products were stored and handled in a argon-filled glove box because of their sensitivity to oxygen and moisture. The compounds Ba_3I_2Si and Ba_3I_2Ge were prepared by reaction of stoichiometric amounts of barium (Ba rods, ALFA 99.9%, distilled), barium iodide(BaI_2 beads, Aldrich 99.999%), and silicon (Si powder, ALFA 99.9%) or germanium (Ge powder, ALFA 99.9999%) at 1170 K for 8 h in sealed niobium ampoules under vacuum. After cooling down by 50 K/h, samples of Ba_3I_2Si were yielded in fairly high purity (no extra lines in the X-ray pattern), while samples of Ba_3I_2Ge show minor impurities due to contributions of Ba_2Ge. In both cases we obtained a brittle material that shows a black metallic luster, decomposes slowly in air, and reacts violently with water under development of pyrophoric gas. According to differential thermal analysis, Ba_3I_2Si melts congruently at 1110 K.

2.2. Structural Studies

The data collection for Ba_3I_2Si was performed on a bar-shaped single crystal ($\approx 0.2 \times 0.06 \times 0.06$ mm) on a diffractometer with CCD detector (SIEMENS SMART PLATFORM) and monochromated MoK_α radiation. The data were integrated with the SAINT program (45) and corrected for Lorentz factor, polarization, air absorption, and absorption due to path length through the detector face plate. The final cell constants (orthorhombic, $a = 10.057(2)$ Å, $b = 14.064(3)$ Å, $c = 29.526(3)$ Å) were determined on a four-circle diffractometer (STOE STADIP) using 41 reflections n the range $33.62^\circ \leq 2\theta \leq 47.68^\circ$. The observed Laue symmetry *mmm* and the extinctions are consistent with the space group *Fddd*. The structure of Ba_3I_2Si was solved using direct methods (46). The final cycle of full-matrix least-squares refinement with 1472 observed reflections ($I > 2\sigma(I)$) and 31 variables (including all positional and anisotropic displacement parameters) converged at $R/R_w = 0.04/0.07$.

The data collection for Ba_3I_2Ge was performed on a bar-shaped single crystal ($\approx 0.2 \times 0.1 \times 0.1$ mm) on an image-plate diffractometer (STOE IPDS) with monochromated MoK_α radiation. The cell constants (orthorhombic, $a = 10.064(2)$ Å, $b = 14.082(2)$ Å, $c = 29.605(3)$ Å) were determined on a four-circle diffractometer(STOE STADIP) using 46 reflections in the range $32.86^\circ \leq 2\theta \leq 46.40^\circ$. The observed Laue symmetry *mmm* and the extinctions are consistent with the space group *Fddd*. The structure of Ba_3I_2Ge was refined using the positional parameters of Ba_3I_2Si as a start model. The final cycle of full-matrix least-squares refinement with 1172 observed reflections ($I > 2\sigma(I)$) and 31 variables (including all positional and anisotropic displacement parameters) converged at $R/R_w = 0.03/0.07$. Atomic coordinates and further details of the structure investigations are listed in Tables 1 and 2. Structure factor tables and further information may be obtained upon request.[3]

2.3. Physical Properties

Conductivity measurements on Ba_3I_2Si were performed on green compacts of the powdered material in a temperature range between room temperature and 450 K. To reduce effects of grain boundaries in the conductivity measurements, the pills (diameter, 6 mm; thickness, 0.8 mm) were heated up to 1070 K for another 10 h in niobium ampoules. Based on the van der Pauw method (47) rhodium electrodes in a square arrangement were pressed against the plane surface of the pill (48). Two electrodes were used to

[2] Beside halogenide silicides, other examples of compounds containing halogenides and Zintl anions exist, which may interpreted as double salts, too; see, e.g., (41).

[3] See NAPS document No. 05550 for 9 pages of supplementary material. Order from NAPS c/o Microfiche Publications, 248 Hempstead Turnpike, West Hempstead, NY 11552. Remit in advance in U.S. funds only $15.00 for photocopies or $5.00 for microfiche. There is a $25.00 invoicing charge on all orders filled before payment. Outside U.S. and Canada please add $4.50 for the first 20 pages and $1.00 for each 10 pages of material thereafter, or $5.00 for the first microfiche and $1.00 for each microfiche therefore.

TABLE 1

Empirical formula	Ba_3I_2Si	Ba_3I_2Ge
Formula weight	693.91	738.41
Space group	*Fddd*	*Fddd* (No. 70)
Volume [10^3 Å^3]	4176(2)	4196(2)
Unit cell dimensions [Å]	$a = 10.057(2)$	$a = 10.064(2)$
	$b = 14.064(3)$	$b = 14.082(2)$
	$c = 29.526(3)$	$c = 29.605(3)$
Formula units/cell	16	16
Density ρ_{calc} [g cm^{-3}]	4.415	4.676
μ(Mo$K\alpha$) [mm^{-1}]	17.134	19.749
θ_{max} [deg]	33.28	27.99
Index range	$-14 \le h \le 14$,	$-13 \le h \le 13$,
	$-21 \le k \le 21$,	$-18 \le k \le 18$,
	$-45 \le l \le 44$	$-35 \le l \le 34$
Independent reflections		
$R_{int.}$ [a]	1941, 0.09	1206, 0.08
R/R_w [b,c] [$I > 2\sigma(I)$]	0.04/0.07	0.03/0.07
R/R_w (all data)	0.07/0.08	0.03/0.07

[a] $R_{int} = (\sum F_0^2 - \bar{F}_0^2)/\sum F_0^2$.
[b] $R = \sum(F_0 - \bar{F}_c)/\sum F_0$.
[c] $R_w = \sqrt{\sum(w(F_0^2 - \bar{F}_c^2)^2)/\sum w(F_0^2)^2}$
$w = \dfrac{1}{[\sigma^2(F_0^2) + (gP)^2 + kP)]}$, $P = (\mathrm{Max}(F_0^2, 0) + 2F_c^2)/3$, k, g = weights.

apply a constant current the other two to measure the voltage changes.

From the temperature dependence of the electrical resistivity (Fig. 1) a semiconducting behavior with a bandgap of ≈ 0.4 eV is deduced.

Isotropic susceptibility measurements on the pure phase Ba_3I_2Si were performed in the temperature range of 2 to 293 K using a SQUID magnetometer (MPMS 5S, Quantum Design) in a field of 10 kG. A Suprasil tube of 5 mm diameter was used as sample holder. The material was found to be diamagnetic with a mol susceptibility of $\simeq -7.7 \times 10^{-5}$ cm^3/mol at 293 K (Fig. 2). The value is corrected experimentally with respect to the diamagnetic contribution of the sample holder.

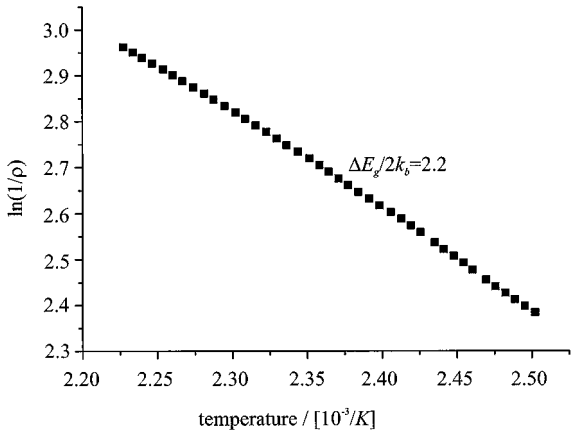

FIG. 1. Temperature dependence of the specific resistance ρ (in [Ω cm]) of Ba_3I_2Si .

2.4. Theoretical Studies

The band structure calculations on Ba_3I_2Si were performed using the tight-binding Linear Muffin Tin Orbital method in the atomic sphere approximation (TB-LMTO-ASA (49)). The calculations are based on density functional theory with a local exchange-correlation potential due to Barth and Hedin (50) and an additional nonlocal exchange-correlation potential due to Perdew and Wang (51). The radii of the overlapping muffin-tin spheres in the ASA approximation are chosen following the suggestions outlined by Jepsen and Andersen (52, 53). The basis consists of Si-3(*s*,*p*), Ba-5*s*, Ba-5*d*, I-5*p*, and 1*s* partial waves for interstitial spheres with I-6*s*, Ba-5*p*, and 2*p* partial waves of the interstitial folded down into the tails of the resulting muffin tin orbitals (54). The I-5*s* function is treated as core function.

TABLE 2
Atomic Coordinates and Displacement Parameters for Ba_3I_2Si(I) and Ba_3I_2Ge(II)

Atom		x	y	z	U_{11}	U_{22}	U_3	U_{23}	U_{13}	U_{12}	U_{eq}
Ba(1)	I	0.8339(1)	$\frac{1}{8}$	$\frac{1}{8}$	186(2)	190(3)	181(3)	1(2)	0	0	186(1)
	II	0.8347(1)	$\frac{1}{8}$	$\frac{1}{8}$	194(3)	211(2)	243(3)	−4(1)	0	0	216(2)
Ba(2)	I	0.6407(1)	0.3560(1)	0.0340(1)	214(2)	174(2)	197(2)	1(1)	21(1)	−3(1)	195(1)
	II	0.6405(1)	0.3564(1)	0.0341(1)	225(2)	202(2)	257(2)	−1(1)	23(1)	0(1)	228(1)
I(1)	I	$\frac{1}{8}$	$\frac{1}{8}$	0.0481(1)	225(3)	323(4)	278(3)	0	0	24(3)	275(2)
	II	$\frac{1}{8}$	$\frac{1}{8}$	0.0480(1)	242(3)	346(3)	340(3)	0	0	24(2)	309(2)
I(2)	I	$\frac{1}{8}$	$\frac{1}{8}$	0.8793(1)	312(3)	209(3)	252(3)	0	0	53(3)	258(2)
	II	$\frac{1}{8}$	$\frac{1}{8}$	0.8792(1)	329(4)	237(3)	309(3)	0	0	56(2)	292(2)
Si	I	$\frac{1}{8}$	$\frac{1}{8}$	0.7092(1)	197(12)	187(12)	192(11)	0	0	12(9)	192(5)
Ge	II	$\frac{1}{8}$	$\frac{1}{8}$	0.7091(1)	209(5)	203(4)	228(4)	0	0	18(2)	213(2)

Note. U_{eq} is defined as one-third of the trace of the orthogonalized $\mathbf{U}_{ij}$ tensor. The components of the anisotropic displacement tensor are defined for $\exp[-2\pi^2(U_{11}h^2a^{*2} + \cdots + 2U_{23}klb^*c^*)]$.

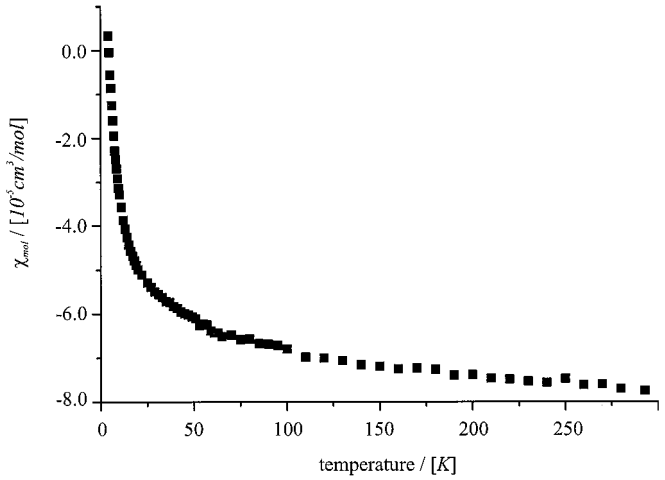

FIG. 2. Temperature dependence of the magnetic mol susceptibility χ_{mol} of Ba_3I_2Si.

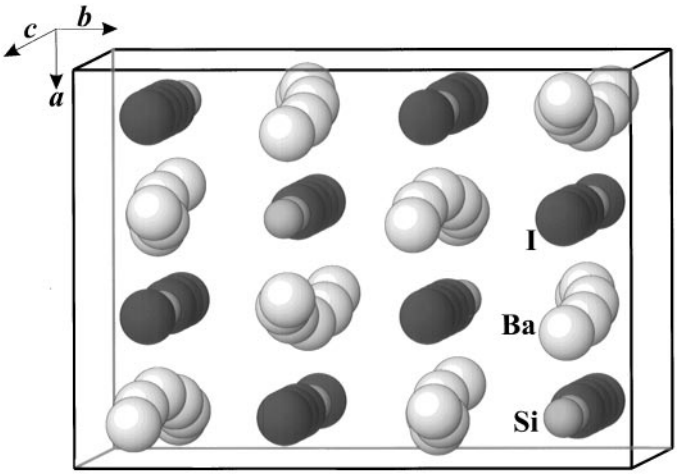

FIG. 3. Perspective view on the structure of Ba_3I_2Si along the c direction (large white spheres, Ba; large black spheres, I; small grey spheres, Si).

The energy expansion parameters $E_{v,RL}$ are chosen at the centers of gravity of the occupied part of the partial state densities. The k space integrations were performed on a set of 171 irreducible k points.

3. RESULTS AND DISCUSSION

The compounds Ba_3I_2Si and Ba_3I_2Ge are isotypic and crystallize in a novel structure type which is based on the rock salt type. The structures are built of isolated barium, iodine, and silicon or germanium atoms, respectively. The distances of 3.24–3.26 Å for Ba–X (X = Si, Ge) and 3.55–3.81 Å for Ba–I in Ba_3I_2Si (cf. Table 3) are comparable to those found in BaI_2 (42), Ba_2Si (43), and Ba_2Ge (44). The structures can be described as an only weakly distorted cubic close packing of iodide and silicon or germanium anions with barium cations occupying all octahedral holes and vice versa. Two neighboring vertices of the octahedra are always occupied by silicon or germanium anions. Due to different size requirements, formal charges and polarizabilities of I^- and Si^{4-} or Ge^{4-} ions the barium cations are slightly shifted out of the octahedral sites toward the silicon edges. Thus, viewing the structure along the c axis a nearly helical distribution of barium cations arises (cf. Fig. 3).

A similar though distinct rock salt based structure type was already suggested for the hypothetical homologue compound Ca_3SiBr_2 by Jansen and Schön (55). Compared to the latter we find a different ordering of the anions. This difference may be illustrated best if we describe the structure

TABLE 3

Atom pair	d	n	Atom pair	d	n
Ba1–Si	325.47(2)	2	I1–Ba1	370.84(7)	2
–I2	354.26(6)	2	–Ba2	380.92(8)	2
–I1	370.53(7)	2			
			I2–Ba1	354.26(6)	2
Ba2–Si	323.94(2)		–Ba2	368.10(7)	2
–Si	325.94(7)		–Ba2	371.10(7)	2
–I1	361.67(7)				
–I2	368.10(7)		Si–Ba2	323.93(2)	2
–I2	371.10(7)		–Ba2	325.46(2)	2
–I1	380.91(8)		–Ba1	325.93(2)	2
			–Si	494.9(2)	2
I1–Ba2	361.66(7)	2	–Si	497.2(5)	

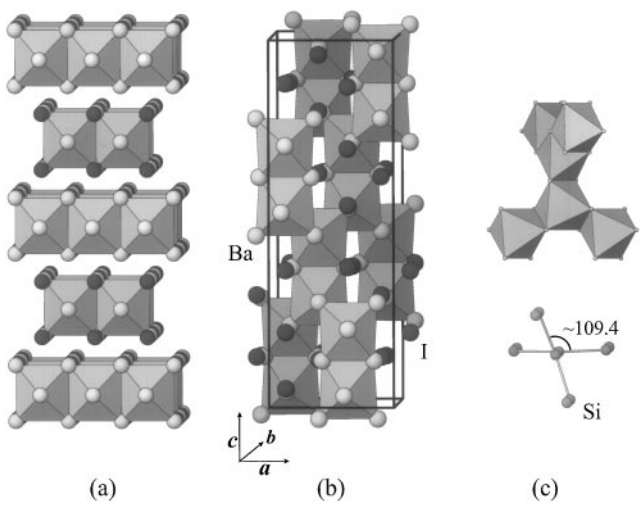

FIG. 4. Comparison between (a) a structure model based on a hypothetical Ca_3SiBr_2 (55) and (b) the crystal structure of Ba_3I_2Si. The packing of Ba_6Si octahedra is emphasized; (c) characteristic building unit of the three-dimensional network in (b) comparable to the Si network in $ThSi_2$.

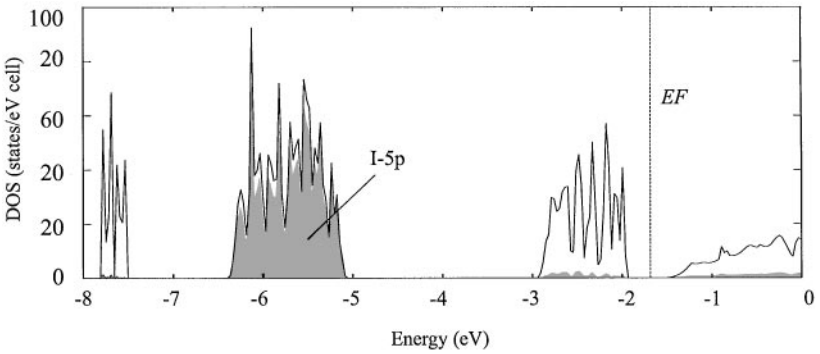

FIG. 5. Electronic density of states (DOS) of Ba_3I_2Si based on an LMTO band structure calculation (contribution of I-5*p* states to the DOS are shown in gray).

by a packing of edge sharing Ba_6 octahedra and focus on the distribution of those octahedra which are centered by silicon anions (cf. Fig. 4a, b).

In the suggested structure model for Ca_3SiBr_2 the silicon anions are distributed in layers, thus each Ba_6Si octahedron shares edges with two as well as vertices with another two neighboring Ba_6Si octahedra (55).[4] Different to this suggestion, in the structure of Ba_3I_2Si each Ba_6Si octahedron shares edges with three neighboring Ba_6Si octahedra. By connecting the octahedral centers or the silicon atoms, a three-connected topology similar to the silicon network in $ThSi_2$ arises (cf. Fig. 4c). Due to the packing of edge sharing octahedra the deltahedral angle between two three-connected Si units is about 109.4° while in $ThSi_2$ 90° are realized. The similarity to $ThSi_2$ is surprising since there are obviously no covalent interactions between the silicon centers taking into account the interatomic distances of 4.95 Å.

LMTO band structure calculations support the ionic picture of the compound. We find Ba_3I_2Si to be a semiconductor with a direct band gap of about 0.4 eV (cf. Fig. 5). The silicon 3*s* and 3*p* states as well as the iodine 5*p* states are fully occupied and dominate the electronic band structure below the Fermi level. Thus, with respect to the character of the occupied states it is obvious to classify Ba_3I_2Si in terms of a *double salt*: $(Ba^{2+})_3(I^-)_2(Si^{4-})$.

This picture is in accordance with the temperature behavior of the electric conductivity which shows Ba_3I_2Si to be semiconducting with a band gap of ≈ 0.4 eV. Measurements of the magnetic susceptibility on Ba_3I_2Si point to a diamagnetic behavior with a mol susceptibility of 7.7×10^{-5} cm^3/mol. However, if one takes into account the diamagnetic increments for Ba^{2+} and I^- of -28×10^{-6} or -57×10^{-6} cm^3/mol, which work well for the interpretation of the magnetism in ionic compounds (e.g., the halogenides of the alkaline earth metals (57, 58)), the absolute value for the mol susceptibility appears too small, even without considering the contributions of a silicon anion. This may be due to minor paramagnetic impurities in the samples. To clear up this topic, more comprehensive studies are in progress.

Further investigations on this class of compounds led to characterization of the compounds Ba_3Br_2Si and Sr_3I_2Si (59), which crystallize in the the same structure type as Ba_3I_2Si. This emphasizes the extraordinary stability of the novel structure type.

[4] In the meantime Jansen *et al.* suggested further NaCl-based structure models for Ca_3SiBr_2, which are not discussed in the present paper (56).

REFERENCES

1. E. Mooser and W. B. Pearson, "Progress in Semiconductors," Band 5. Wiley & Sons Inc., New York, 1960.
2. W. Klemm, "Festkörperprobleme," Band Bd. III. Vieweg, Braunschweig, Germany, 1963.
3. E. Busmann, *Z. Anorg. Allg. Chem.* **313,** 90 (1961).
4. W. Klemm and E. Busmann, *Z. Anorg. Allg. Chem.* **319,** 297 (1963).
5. S. Wengert, Doktorarbeit. ETH Zürich, 1997.
6. R. Ramírez, R. Nesper, H. G. v. Schnering, and M. Böhm, *Chem. Phys.* **95,** 17 (1985).
7. R. Ramírez, Doktorarbeit. Universität Stuttgart, 1986.
8. E. Zintl, J. Goubeau, and W. Dullenkopf, *Z. Phys. Chem.* **A154,** 1 (1931).
9. E. Zintl and H. Kaiser, *Z. Anorg. Allg. Chem.* **211,** 113 (1933).
10. J. D. Corbett, *Chem. Rev.* **85,** 383 (1985).
11. H. Ansari and J. Ibers, *Coord. Chem. Rev.* **100** (1990).
12. J. D. Corbett, *Angew. Chem., Int. Ed. Engl.* **32,** 1646 (1993).
13. J.-S. Jung, B. Wu, L. Ren, J. Tang, J. Ferre, J. Jamet, and C. J. O'Connor, *J. Mater. Res.* **9,** 909 (1994).
14. N. Korber and J. Daniels, *Helv. Chim. Acta* **79,** 2083 (1993).
15. N. Korber and F. Richter, *Angew. Chem.* **36,** 1512 (1997).
16. T. F. Fässler and M. Hunziker, *Z. Anorg. Allg. Chem.* **622,** 837 (1985).
17. H. Siegl, W. Krumlacher, and K. Hassler, *Monatsh. Chem.* **130,** 139 (1999).
18. J. B. K.-Th. Wilke, "Kristallzüchtung." Verlag Harry Deutsch, Thun, Germany, 1988.
19. H. M. Haendler, P. M. Carknerxi, S. M. Boudreau, and R. A. Boudreau, *J. Solid State Chem.* **29,** 35 (1979).
20. M. H. Möller and W. Jeitschko, *J. Solid State Chem.* **65,** 178 (1986).
21. W. Milius and A. Rabenau, *Z. Naturforsch. B* **43,** 243 (1988).

22. W. Milius, *Z. Anorg. Allg. Chem.* **586,** 175 (1990).
23. A. Pfitzner and S. Zimmerer, *Z. Anorg. Allg. Chem.* **621,** 969 (1995).
24. A. Pfitzner and E. Freudenthaler, *Angew. Chem.* **34,** 1647 (1995).
25. A. Pfitzner and S. Zimmerer, *Z. Anorg. Allg. Chem.* **622,** 853 (1996).
26. A. Pfitzner and E. Freudenthaler, *Z. Naturforsch. B* **52,** 199 (1997).
27. E. Freudenthaler and A. Pfitzner, *Solid State Ionics* **101,** 1053 (1997).
28. W. Sundermeyer, *Angew. Chem.* **77,** 241 (1965).
29. A. v. Rumohr, W. Sundermeyer, and W. Towae, *Z. Anorg. Allg. Chem.* **499,** 75 (1983).
30. H.-J. Klockner and W. Sundermeyer, *Z. Anorg. Allg. Chem.* **509,** 76 (1984).
31. H. Liesenhoff and W. Sundermeyer, *Z. Naturforsch. B* **54,** 573 (1999).
32. C. R. Boston, *in* "Advances in Molten Salt Chemistry," Vol. 1, Chap. 3, pp. 126–163. Plenum Press, New York, 1971.
33. H. L. Jones and R. A. Osteryoung, *in* "Advances in Molten Salt Chemistry," Vol. 3, Chap. 3, pp. 121–176. Plenum Press, New York, 1975.
34. T. Welton, *Chem. Rev.* **99,** 2071 1999.
35. F. Rohrer, Doktorarbeit. ETH Zurich, 1997.
36. F. E. Rohrer and R. Nesper, *J. Solid State Chem.* **135,** 194 (1998).
37. F. E. Rohrer and R. Nesper, *J. Solid State Chem.* **142,** 187 (1999).
38. M. Pell and R. Nesper, unpublished (1997).
39. A. Simon and H. Mattausch, *Angew. Chem.* **110,** 499 (1998).
40. H. Mattausch, O. Oeckler, and A. Simon, *Z. Anorg. Allg. Chem.* **625,** 1 (1999).
41. G. Gauthier, S. Kawasaki, S. Jobic, P. Macaudiere, R. Brec, and J. Rouxel, *J. Alloys Comp.* **275–277,** 46 (1998).
42. E. B. Brackett and T. E. Brackett, *J. Phys. Chem. A* **67,** 2132 (1963).
43. G. Bruzzone and E. Franceschi, *J. Less Common Met.* **57,** 201–208 (1978).
44. K. Turban and H. Schäfer, *Z. Naturforsch. B* **28,** 220 (1973).
45. SAINT Version 4.05. Siemens Analytical X-ray Instruments, Madison, WI, 1996.
46. SHELXTL, Version 5.1. Bruker AXS, Inc., Madison, WI, 1997.
47. L. J. van der Pauw, *Philips Res. Rep* **13,** 1 (1958).
48. C. Mensing and R. Nesper, "Messzelle zur Bestimmung der spezifischen Leitfähigkeit nach van der Pauw." ETH Zürich, 1995.
49. G. Krier, O. Jepsen, A. Burkhardt, and O. K. Andersen, "TB-LMTO-ASA Program." Stuttgart, 1994.
50. U. Bart and L. Hedin, *J. Phys. C* **5,** 1629 (1972).
51. J. P. Wang and Y. Wang, *Phys. Rev. B* **45,** 13244 (1992).
52. LMTO data for Ba_3I_2Si: 171 irreducible k points, Ba1(3.36[a]), Ba2(3.33), I1(3.51), I2(3.34), Si1(2.80), E(2.29//-.3835, 0.0020, -.2113[b]), E1(2.21// $-\frac{1}{8}$, 0.0174, $-\frac{1}{8}$), E2(2.16// -0.3621, -.2543, -.2006), E3(2.18// $-\frac{1}{8}$, -0.4800, $-\frac{1}{8}$); [a]muffin tin radius in Å; [b]fractional coordinates.
53. O. Jepsen and O. K. Andersen, *Z. Phys. B* **97,** 35 (1995).
54. W. R. L. Lambrecht and O. K. Andersen, *Phys. Rev. B* **34,** 2439 (1986).
55. J. Schön and M. Jansen, *Angew. Chem.* **108,** 1358 (1996).
56. H. Putz, J. Schön, and M. Jansen, *Z. Anorg. Allg. Chem.* **625,** 1624 (1999).
57. W. Klemm, *Z. Anorg. Allg. Chem.* **240,** 377 (1940).
58. W. Klemm, *Z. Anorg. Allg. Chem.* **244,** 347 (1941).
59. S. Wengert and R. Nesper, *Z. Kristallogr.* NCS, in preparation.